Neuro-Oncology 12(1):58–70, 2010.
doi:10.1093/neuonc/nop013

Osteopontin regulates human glioma cell invasiveness and tumor growth in mice

Hsun-Jin Jan, Chin-Cheng Lee, Yung-Luen Shih, Dueng-Yuan Hueng, Hsin-I Ma, Jing-Huei Lai, Hen-Wei Wei, and Horng-Mo Lee

Graduate Institute of Medical Sciences, Taipei Medical University, Taipei, Taiwan (H.-J.J., J.-H.L., H.-M.L.); Department of Pathology, Shin Kong Memorial Hospital, Taipei, Taiwan (C.-C.L., Y.-L.S.); Department of Neurosurgery, Tri-services General Hospital, Taipei, Taiwan (D.-Y.H., H.-I.M.); Department of Animal Science and Technology, National Taiwan University, Taipei, Taiwan (H.-W.W.); Institute of Pharmaceutical Technology, Central Taiwan University of Technology, Taichung, Taiwan (H.-M. L.)

Human malignant glioma cells are characterized by local invasion. In the present study, we investigated the role of osteopontin (OPN) in the invasiveness of human glioma cells isolated from grade IV tumors. We found that the expression levels of OPN in these cell lines paralleled matrix metalloproteinase-2 (MMP-2) expression and cell invasiveness potential. When U87MG glioma cells (with a high-OPN expression level) were stably transformed with specific small hairpin RNA to knock down OPN expression, MMP-2 secretion, cell invasiveness, and tumor growth in implanted brains were dramatically reduced. Conversely, forced expression of OPN in GBM-SKH glioma cells (which expressed OPN at a low level) increased MMP-2 secretion, enhanced cell invasiveness, and increased tumor growth in a rodent xenograft model. Expression of OPN was associated with increased expression of vimentin and decreased expression of glial fibrillary acidic protein. Treatment of glioma cells with 5-aza-2′-deoxycytidine (5-aza-dC) suppressed OPN expression in a concentration-dependent manner. Suppression of OPN expression by 5-aza-dC was associated with reductions in MMP-2 secretion, vimentin expression, cell invasion, intravasation, and tumor growth. These data suggest that OPN may play important roles in regulating cell invasion in glioma cells and that 5-aza-dC may serve as a therapeutic agent for human gliomas.

Received September 8, 2008; accepted December 31, 2008.

Corresponding Author: Horng-Mo Lee, PhD, Graduate Institute of Medical Sciences, Taipei Medical University, 250 Wu-Hsing Street, Taipei 110, Taiwan (leehorng@tmu.edu.tw).

Keywords: 5-aza-2′-deoxycytidine, glioma, invasion, MMP-2, osteopontin

Human malignant glioma cells are characterized by uncontrolled growth and rapid invasion of adjacent tissues. The standard treatment regimen includes surgical debulking, radiation therapy, and cytotoxic chemotherapy using temozolomide. However, the prognosis for gliomas remains poor with only 5% of patients with a 5-year survival rate despite maximal therapy.[1–3] Because current therapies fail to control gliomas from invading contiguous normal brain tissues, recent drug developments have focused on controlling the invasive capability of gliomas. Malignant glioma cells express certain known proteinases such as matrix metalloproteinases (MMPs), which have been implicated as important factors in regulating cell invasiveness and angiogenesis in gliomas.[4] MMPs constitute a family of enzymes with 25 members and 3 pseudo-MMPs, which are extracellular endopeptidases requiring metal ions for their enzymatic activity. Among the MMPs, attention has focused on gelatinases (MMP-2 and MMP-9) in human gliomas. A high level of MMP-2 expression was observed in the higher-grade gliomas, which correlated well with the malignant potential of human gliomas.[5]

Osteopontin (OPN) is a non-collagenous, sialic acid-rich, and glycosylated phosphoprotein secreted by the osteoid matrix, which regulates osteoblast function during bone formation.[5] In addition to bone remodeling, OPN is also present in a variety of tissues and plays important roles in inflammation, immune responses, and biomineralization. OPN mediates cell adhesion, migration, and invasion in a wide range of tumor cells.[6–9] OPN is predominantly observed in the microvasculature of glioblastomas and is implicated as an

important molecule in angiogenesis.[10] OPN is one of the hypoxia-related genes, induced by hypoxia *in vitro* and *in vivo*.[11] A suppression subtractive hybridization study revealed that OPN plays crucial roles in brain invasion.[12] OPN expression is implicated in the malignancies of human malignant gliomas and is the most up-regulated gene in the *N*-ethyl-nitrosourea-induced glioma model in rats.[13–16] OPN is shown to regulate MMP-2 expression and cell invasiveness in melanoma cells.[17,18] Knockdown of OPN mRNA by small interfering RNA significantly attenuates tumor cell motility and invasiveness in CT26 colon cancer cells.[19]

Vimentin is an intermediate filament protein, which is up-regulated in highly infiltrative gliomas with poor prognosis. Increased expression of vimentin is linked to malignant tumor progression in melanomas and a variety of cancers.[20–23] Vimentin is up-regulated in progressive malignant gliomas under temozolomide treatment or combined radiotherapy and chemotherapy and is postulated to be a marker of a higher invasive phenotype.[24,25] In addition to vimentin expression, malignant progression of neoplastic astrocytes is accompanied by a decrease in glial fibrillary acidic protein (GFAP) expression. GFAP is an intermediate filament protein that is largely specific for astrocytes and is among the best markers of astrocytic differentiation.[26] GFAP is expressed in pilocytic astrocytoma and has been considered a marker that accurately distinguishes pilocytic astrocytoma from glioblastoma.[12]

In the present study, we investigated the roles of OPN in MMP-2 production, cell invasiveness, and the expressions of vimentin and GFAP in human glioma cells, and we demonstrate that OPN plays an important role in glioma cell invasion by enhancing MMP-2 secretion and vimentin expression in glioma cells. 5-Aza-2′-deoxycytidine (5-aza-dC) is an anticancer drug, currently used in the therapy of acute myeloid leukemia and other myelodysplastic syndromes.[27,28] 5-Aza-dC also inhibits human medulloblastoma cell proliferation and induces tumor cell apoptosis in glioma cells.[29,30] In this report, we provide evidence that 5-aza-dC may regulate MMP-2 and vimentin expression through OPN expression in human glioma cells. We demonstrated that intraperitoneal administration of 5-aza-dC significantly reduced the tumor size in mice with intracranially implanted tumors. These data suggest that 5-aza-dC may be used as a therapeutic agent for gliomas by reducing cell invasiveness through suppression of OPN expression.

Materials and Methods

Materials

Dulbecco's modified Eagle's medium (DMEM), fetal calf serum (FCS), glutamine, gentamycin, penicillin, and streptomycin were purchased from Life Technologies (Gaithersburg, Maryland). Antibody specific for MMP-2 was purchased from Sigma-Aldrich Chemical (St Louis, Missouri). Anti-OPN and anti-α-tubulin antibodies were purchased from Santa Cruz Biotechnology (Santa Cruz, California). Horse-radish peroxidase (HRP)-conjugated anti-rabbit IgG antibody was purchased from Bio-Rad (Hercules, California). The RNAsin ribonuclease inhibitor and Moloney murine leukemia virus reverse transcriptase (RT) were purchased from Promega (Madison, Wisconsin). Protease inhibitor cocktail tablets were purchased from Boehringer Mannheim (Mannheim, Germany). Human U87MG cells (American Type Culture Collection no. HTB-14) were purchased from the Institute of Food Sciences (Hsinchu, Taiwan). GBM-SKH cells were isolated from a grade IV human glioma by C.-C.L. of Shin Kong Memorial Hospital (Taipei, Taiwan). GBM8401 cells were isolated from a grade IV human glioma by H.-I.M. of Tri-services General Hospital (Taipei, Taiwan).

Culture of Human Glioma Cells and Preparation of Cell Lysates

U87MG cells and cell lines derived from human glioma biopsies were cultured in DMEM supplemented with 13.1 mM $NaHCO_3$, 13 mM glucose, 2 mM glutamine, 10% heat-inactivated FCS, and penicillin (100 U/mL)/streptomycin (100 mg/mL). Cultures were maintained in a humidified incubator with 5% CO_2 at 37°C. After reaching confluence, cells were treated with various concentrations of 5-aza-dC and incubated in a humidified incubator at 37°C for the indicated time-intervals. At the end of incubation, cells were lysed by adding lysis buffer containing 10 mM Tris–HCl (pH 7.5), 1 mM EGTA, 1 mM $MgCl_2$, 1 mM sodium orthovanadate, 1 mM DTT, 0.1% mercaptoethanol, 0.5% Triton X-100, and protease inhibitor cocktails, then stored at −70°C for further determinations.

Sodium Dodecyl Sulfate Polyacrylamide Gel Electrophoresis and Western Blotting

Proteins were separated by sodium dodecyl sulfate polyacrylamide gel electrophoresis. After electrophoresis, proteins on the gel were electrotransferred onto a polyvinyldifluoride (PVDF) membrane. After transfer, the PVDF membrane was washed once with PBS and twice with PBS plus 0.1% Tween 20 (PBST). The PVDF membrane was then blocked with blocking solution containing 5% non-fat dry milk in PBST for 1 hour at room temperature. The PVDF membrane was blotted with primary antibodies in the blocking buffer, and then washed again in PBST. The PVDF membrane was incubated with peroxidase-linked anti-mouse immunogliobin G antibodies for 1 hour and then developed by an enhanced chemiluminescence plus detection kit (Amersham Life Sciences, Piscataway, New Jersey), and the relative photographic density was quantitated by scanning the photographic negatives on a gel analysis system (BioSpectrumAC Imaging System Vision Work LS software, UVP Inc., Upland, California).

Gelatin Zymography

Gelatinolytic zymography was used to detect the secretion of MMP-2 in the culture media. Briefly, the

collected media (15 μL) after treatment were loaded onto 10% SDS–PAGE co-polymerized with 0.1% gelatin and subjected to electrophoresis at 100 V for 1.5 hours. In order to remove the SDS, the gel was washed twice with a 2.5% Triton X-100 solution for 30 minutes each, rinsed with incubation buffer (0.05 M Tris–HCl buffer [pH 8.0], 5 mM $CaCl_2$, and 5 μM $ZnCl_2$), and incubated at 37°C overnight. The gel was then stained with a solution of 0.25% Coomassie blue R250, 40% methanol, and 10% acetic acid for 2 hours at room temperature and destained with 40% methanol and 10% acetic acid until the lysis bands became clear. Gelatinase activities in the media were detected as unstained gelatin-degraded zones on the gel. The MMP-2-relative photographic density was quantitated by scanning the photographic negatives on a gel analysis system (BioSpectrumAC Imaging System Vision with LS software, UVP Inc.).

Transfection of Plasmids

For OPN knockdown, U87MG cells were seeded at 5×10^5 cells per 6-cm plate and allowed to adhere overnight. The next day, a vector control (plKo) and OPN-specific small hairpin RNA plasmid (shOPN) (oligo sequence: CCGGCCACAAGCAGTCCAGATTATACTCGAGT-ATAATCTGGACTGCTTGTGGTTTTT) were transfected into cells using Lipofectamine 2000 (Invitrogen). After 24 hours, transfected cells were split equally into 6-cm plates and allowed to adhere overnight. For OPN overexpression, GBM-SKH cells were seeded at 5×10^5 cells in a 6-cm plate. Next day, pcDNA3.1/OPN (accession no. NM_000582) or the control pcDNA3.1 vector was transfected. After 24 hours, the medium was changed to select G418-resistant clones.

In Vitro *Matrigel Invasion Assay (Boyden Chamber)*

In vitro invasion of glioma cells was measured using Matrigel-coated transwell inserts (BD Biosciences, Mansfield, Massachusetts). Briefly, glioma cells (2×10^5) pretreated under the indicated conditions were suspended in serum-free DMEM in the upper wells and allowed to transmigrate through the membrane inserts toward the lower wells that were filled with DMEM containing 10% FCS. At the end of incubation, non-invading cells on the upper side of the membrane were gently removed using a cotton-tipped swab. Cells which had migrated to the lower side of the membranes were fixed, stained with toluidine blue solution (Sigma-Aldrich), and counted.

Total RNA Isolation and RT-Polymerase Chain Reaction

Total RNA was extracted from cultured glioma cells using TRIzol reagent (Invitrogen). Two micrograms of total RNA were used for cDNA synthesis by RT. The reaction was carried out in a 20-μL reaction mixture containing 1 μg of total cellular RNA, 1× buffer (50 mM Tris [pH 8.3], 61.5 mM KCl, and 3 mM $MgCl_2$); 1 mM each of dATP, dTTP, dGTP, and dCTP, 20 pmol of a random hexamer, and 200 U of RT (Superscript II Rnase H^-, Gibco BRL, Carlsbad, California) at 25°C for 10 minutes and then at 42°C for 50 minutes. The reaction was stopped by incubating the reaction mixture at 70°C for 15 minutes. Primers for MMP-2 (forward: 5′-GAGTTGGCAGTGCAATACC T-3′; reverse: 5′-GCCGTCCTTCTCAAAGTTGT-3′), OPN (forward: 5′-GAAAGCGAGGAG TTGAATGG -3′; reverse: 5′-TTCCATGAAGCCACAAACTA-3′), and glyceraldehyde-3-phosphate dehydrogenase (forward: 5′-GCCAAAAGGGTCATCATCTCTG-3′; reverse: 5′-C ATGCCAGTGAG CTTCCCGT-3′) were derived from human cDNA sequences, and polymerase chain reaction (PCR) conditions were optimized so that the gene products were in the exponential phase of amplification (94°C for 2 minutes, then for 30 cycles at 94°C for 30 s, 55°C for 1 minutes, and 72°C for 1 minute, followed by a final elongation for 7 minutes at 72°C). PCR products were resolved on 1.5%–2% agarose gels containing 1 μg/mL ethidium bromide.

In Vivo *Intravasation Assay*

The chorioallantoic membrane (CAM) intravasation assay was carried out according to Kim *et al.*[31] with few modifications. Chicken embryos at 10 days of gestation were incubated in a rotary incubator at 38°C with 60% humidity. A small hole was drilled into the top of the egg above the area of greatest vasculature, causing the CAM to detach from the shell membrane. Human glioma cells (10^5), in a volume of 50 μL of complete corresponding enzymatic-free cell culture media, were inoculated onto the dropped CAM with a pipette tip (5 eggs for each tumor type). The holes were sealed with tape, and the eggs were returned to the incubator. Ten days after inoculation (day 14), the eggs were carefully opened. The CAMs lining the cavity of the eggshell were removed, snap-frozen, and used for the extraction of genomic DNA. The frozen CAMs were crushed to a powder, suspended in digestion buffer (100 mM NaCl, 10 mM Tris–Cl [pH 8.0], 25 mM EDTA, 0.5% SDS, and 0.1 mg/mL proteinase K), and incubated at 50°C for 18 hours. Genomic DNA in the sample was extracted using the Sigma genomic isolation kit (Sigma Chemical). Intravasation of human glioma cells was demonstrated by the presence of the human *Alu* sequence in the CAM. Human *Alu* sequence was analyzed by a PCR-based assay, which produced an *Alu* band of 224 bp.[31] The PCR products were resolved on a 2% agarose gel containing 1 μg/mL ethidium bromide. The primers for the human *Alu* sequence were forward: 5′-ACGCCTGTAATCCCAGCACTT-3′ and reverse: 5′-TCGCCCAGGCTGGAGTGCA-3′.

Cell Viability Assays

For the dye exclusion assay, cells were seeded at 2.5×10^4 per well in 24-well plates. Media were removed,

and the cells were rinsed with PBS before incubation with trypsin. Cells were then washed, and resuspended in 0.4% trypan blue, and live cells were counted on a hemocytometer. Cell viability was evaluated using an 3-(4,5-dimethylthiazol-2-yl)-2,5-diphenytetrazolium bromide (MTT) assay. Glioma cells grown on the 150-mm plates were washed twice with PBS and resuspended into DMEM. The suspended cells were plated on 24-well plates (2×10^5 cells/well) and treated with the indicated reagent(s) for 24 hours. MTT was added to the medium (1 mg/mL), and cells were incubated at 37°C for 2 hours. Then dimethylsulfoxide (100 μL) was applied to the medium to dissolve the formazan crystals derived from mitochondrial cleavage of the tetrazolium ring of MTT. The absorbency at 570 nm in each well was measured on a micro-enzyme-linked immunosorbent assay plate reader. None of the reagents used in this study interfered with the MTT values.

In Vivo *Intracranial Xenograft Studies*

Cells were freshly prepared and adjusted to 1×10^5 cells/μL before implantation. An intracranial xenograft was performed according to the Institutional Animal Care and Use Committee-approved protocols. Briefly, nude mice were anesthetized and placed in a stereotactic frame, and the skull was exposed by incision. A hole was made 3 mm to the right of the bregma, and cells (5 μL) were injected using a 10-μL Hamilton syringe with a 26S-gage needle mounted in a stereotactic holder. The syringe was lowered to a depth of 3.5 mm and then raised to a depth of 2.5 mm. The glioma cells were injected at a rate of 0.5 μL/10 s. After intracranial implantation, a 5-minute waiting period was observed before slowly withdrawing the syringe to prevent any reflux. The skull was then cleaned, the hole was sealed with bone wax, and the incision was sutured. Tumors were allowed to grow, and animals were sacrificed on day 21, or when the animals developed signs of neurological deficits.[32, 33] Mice were perfused, and the brains were extracted and post-fixed in 4% paraformaldehyde overnight and then embedded in paraffin for further analysis. Formalin-fixed, paraffin-embedded tissue sections were dewaxed in xylene for 10 minutes, rehydrated in alcohol solution, and stained with hematoxylin and eosin (H&E). The size of brain tumors was microscopically determined as described by Ma *et al.*[32, 33] Briefly, all tumors were sectioned through their largest diameter, and representative sections were used for quantitative analyses. The mean values of the sections from three independent experiments in each group were used for the quantitative analyses of tumor sizes.

Administration of 5-aza-dC and Immunohistochemistry

Nude mice implanted intracranially with 5×10^5 human glioma cells were administered 5-aza-dC (3.75 mg/kg) or PBS at 48-hour intervals by an intraperitoneal injection. Mice were sacrificed by cardiac puncture 21 days after implantation. Paraffin sections were prepared for immunohistochemical staining for OPN, GFAP, and vimentin. Briefly, 4–6-μm-thick sections were cut using a microtome and applied to PLL-coated slides. Sections were deparaffinized, rehydrated, and placed in 5% hydrogen peroxide in absolute alcohol for 10 minutes to block the endogenous peroxidase activity. To unmask the antigen by heat treatment, slides were placed in a container, covered with 10 mM sodium citrate buffer (pH 6), and heated to 95°C for 5 minutes. The slides were tapped off with fresh buffer and heated at 95°C for 5 minutes and then allowed to cool in buffer for 20 minutes. Slides were washed in deionized water 3 times, for 2 minutes each, on a stirring plate. All subsequent steps were carried out at room temperature in a humidified chamber. Tissue sections were not allowed to dry out at any time during the procedure. The primary antibody was diluted (1:50) in a sufficient volume to cover the tissue and incubated for 2 hours. Slides were rinsed with PBS and then washed in PBS twice for 2 minutes each on a stirring plate. Sections were incubated for 30 minutes in a biotinylated secondary antibody at a dilution of 1:200. Slides were rinsed with PBS and then washed with PBS twice for 2 minutes each on stir plate. Tissue sections were then incubated with a HRP-streptavidin complex (Dako) for 30 minutes before being washed again with PBS. The immunostaining was visualized by development in diaminobenzidine before being counterstained with Mayer's H&E stain.

Statistical Analysis

Results are expressed as the mean ± standard error of the mean (SEM) from the number of independent experiments performed. One-way analysis of variance (ANOVA) was used to assess the difference of means among groups, and Student's two-tailed *t*-test was used to determine the difference of means between any two groups. A P value of $<.05$ was taken as statistically significant.

Results

OPN Expression Correlates to Increased Invasiveness in Cell Lines Derived from Human Gliomas

Invasive growth of gliomas may be directly related to histologic malignancy, but occurs to some extent irrespective of tumor grade. We first compared the capabilities of invasiveness and proliferation rates of U87MG cells and two other cell lines derived from human grade IV gliomas (GBM-SKH and GBM8401). As shown in Fig. 1A and B, cell invasiveness and proliferation rates were higher in U87MG and GBM8401 cells and lower in GBM-SKH cells. To confirm the differential cell invasiveness of these glioma cells *in vivo*, an intravasation assay based on the CAM model using chicken embryos was carried out. Although GBM-SKH cells

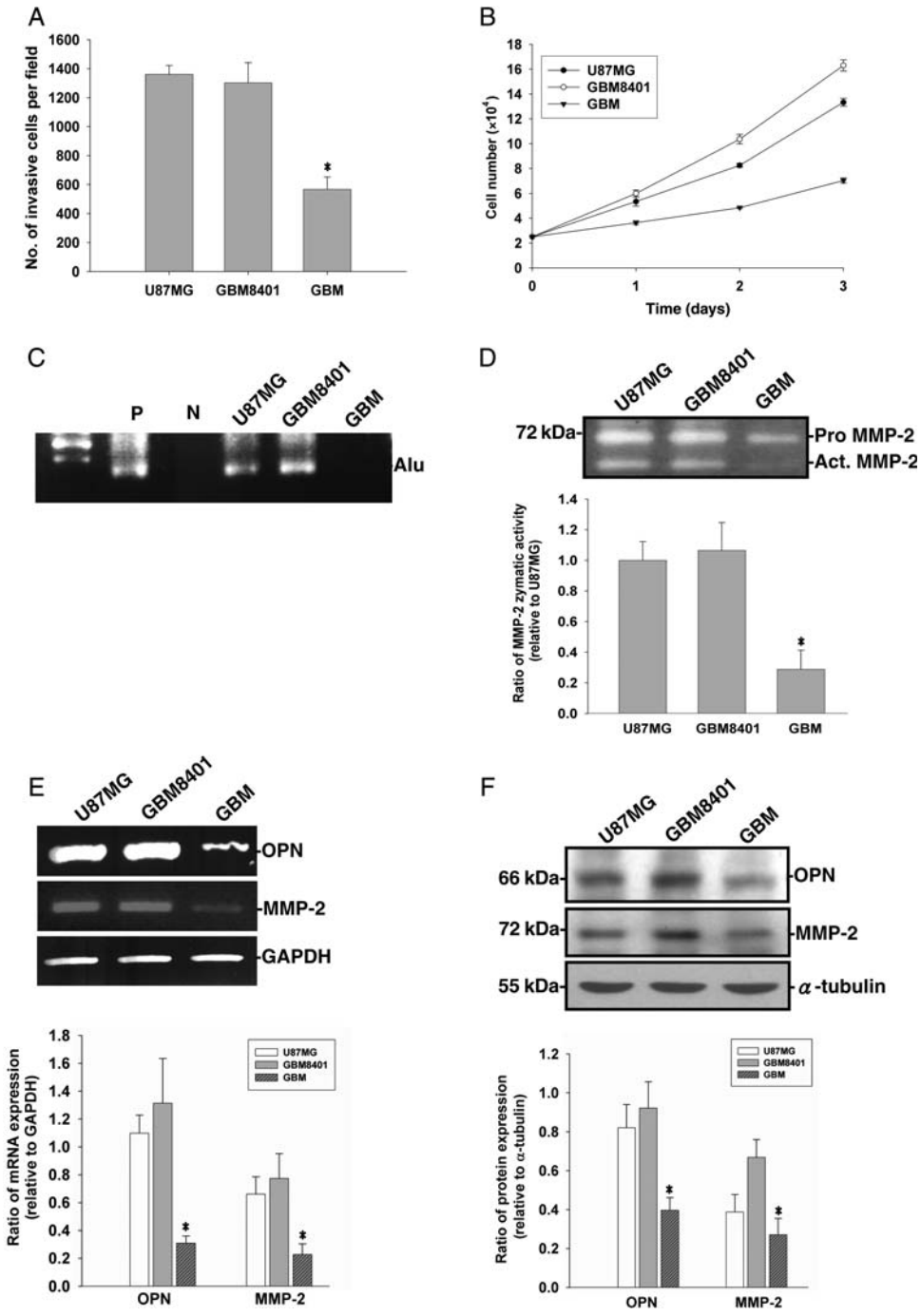

Fig. 1. Cell lines derived from human gliomas exhibit different growth rates, invasiveness, and intravasation. (A) For the *in vitro* invasion assay, equal numbers of glioma cells were seeded in the upper part of a transwell coated with Matrigel. After 24 hours, cells on the bottom side of filter were fixed, stained, and counted. Data represent the mean ± SE of three independent experiments. (B) Viable cell numbers were counted at 24, 48, and 72 hours. Data represent the mean ± SE of three independent experiments. (C) A chicken embryo CAM model was used for the *in vivo* intravasation assay. Intravasation was demonstrated by amplification of the human *Alu* sequence from DNA extracted from the isolated CAMs. P, positive control; N, negative control. (D) Medium was collected and MMP-2 gelatinolytic activities were analyzed by zymography. In the lower panel, the MMP-2 activity was quantitated by scanning the photographic negatives on a gel analysis system. (E) MMP-2, OPN, and glyceraldehyde-3-phosphate dehydrogenase (GAPDH) mRNA expressions were analyzed by RT–PCR. (F) Cell lysates were harvested and immunoblotted with antibodies specific for MMP-2, OPN, and α-tubulin. The upper panels of (E) and (F) are representative data, these experiments were repeated, and the intensities of bands were quantitated and expressed as ratios to equal loading controls. Results shown in the lower panels are the mean ± SE of three independent experiments. *$P < .05$, compared with U87MG.

failed to intravasate into the vasculature of CAM, U87MG and GBM8401 cells exhibited the ability to intravasate (Fig. 1C). Because MMP-2 secretion has been linked to cell invasiveness, we next examined the gelatinolytic activity in cultured media of these cells. Figure 1D shows that the MMP-2 gelatinolytic activities secreted by U87MG and GBM8401 were much higher than those of GBM-SKH cells. OPN has been shown to induce MMP-2 production and activation in many cancer cells and has been correlated with malignancies of gliomas.[6–8] Next, we examined the OPN mRNA and protein expressions in glioma cells. The mRNA expression levels of OPN and MMP-2 were higher in U87MG and GBM8401 cells compared with GBM-SKH cells (Fig. 1E). Similar protein expression patterns of MMP-2 and OPN were found in cell lysates prepared from these cells (Fig. 1F).

OPN Knockdown Suppressed Cell Invasiveness and Tumor Growth in U87MG Glioma Cells

To further examine the role of OPN in cell invasiveness and tumor growth, shRNA specific for OPN was used to knock down OPN expression in the more invasive U87MG cells (that expressed a higher OPN level). Knockdown of OPN expression was demonstrated by suppression of OPN mRNA and protein expression in U87MG cells (Fig. 2A and B). The gelatinolytic activity secreted by U87MG cells was also lowered in OPN-knockdown cells (Fig. 2C). We next determined whether knockdown of OPN altered Matrigel invasion by U87MG cells. As shown in Fig. 2D, knockdown of OPN dramatically reduced cell invasiveness in U87MG cells. To evaluate whether OPN gene expression affects tumor cell proliferation, we examined the number of viable cells using the trypan blue exclusion assay. As shown in Fig. 2E, knockdown of OPN reduced the number of viable cells in U87MG cells. To explore further, we employed an intracerebral xenograft mouse model to investigate tumor growth in nude mice. U87MG cells were either stably transfected with OPN shRNA or a control vector before cell implantation. On day 21 after tumor inoculation, tumor volumes were evaluated in half of the animals. Tumor size was smaller in animals implanted with OPN-knockdown U87MG cells compared with those implanted with control U87MG cells (Fig. 2F).

Increased Expression of OPN-Enhanced Invasiveness by GBM Cells

To further confirm the role of OPN in mediating cell invasiveness and tumor growth, OPN was overexpressed in the less-invasive GBM-SKH glioma cells, and Matrigel invasion and tumor growth in nude mice were examined. As shown in Fig. 3A and B, transfection of an OPN-bearing plasmid increased OPN mRNA and protein levels in GBM-SKH cells. Overexpression of OPN was associated with increased MMP-2 mRNA and protein expressions in the cells (Fig. 3A and B) and gelatinolytic activity in the media of GBM-SKH cultures (Fig. 3C). Overexpression of OPN in GBM-SKH cells also promoted cell invasiveness (Fig. 3D) and the cell proliferation rate *in vitro* (Fig. 3E). To further understand the roles of OPN in glioma tumor growth, nude mice were implanted intracranially with GBM-SKH cells bearing an empty vector or GBM-SKH cells that overexpressed OPN. Tumor size was significantly increased in animals implanted with OPN overexpressing GBM-SKH cells compared with those implanted with control GBM-SKH cells (Fig. 3F). Figure 4 shows a high magnification photo of H&E stain of brain tissue sections. Invasion nests in surrounding brain tissue were noted in mouse brains implanted with the highly invasive U87MG cells but not those implanted with OPN-knockdown U87MG cells. Conversely, invasion nests were noted in OPN-overexpressing GBM-SKH cells, but not in brain tissues grafted with the low-invasive GBM-SKH cells. To demonstrate that tumor invasiveness was associated with OPN overexpression, immunohistochemical staining was performed. The microphotograph shows cytoplasmic staining of OPN in the main tumor mass and invasion nests of tumor cells in rat brain tissues (Fig. 4, right panels). These results suggested that OPN enhanced cell invasiveness *in vivo*.

OPN Regulates Vimentin and GFAP Expressions in Glioma Cells

Increased expression of vimentin and the progressive loss of GFAP are associated with a high degree of invasiveness and tumor growth in human gliomas.[26] To explore the possibility that OPN may contribute to increased vimentin and decreased GFAP expressions, vimentin and GFAP protein levels were examined in cells expressing different OPN levels. As shown in Fig. 5A, U87MG cells expressed low GFAP and high vimentin protein levels. Knockdown of OPN resulted in increased GFAP expression and decreased vimentin expression in U87MG cells. On the other hand, forced expression of OPN in GBM cells (which expressed a low OPN level) slightly decreased GFAP protein expression and increased the vimentin protein level (Fig. 5A, left panel). The *in vitro* data could be replicated in the intracranial xenograft mice model. As shown in Fig. 5B, implantation of OPN-knockdown U87MG/shOPN cells into mouse brains resulted in increased GFAP expression and decreased vimentin expression in brain sections. Consistently, overexpression of OPN in GBM cells led to a slight decrease in GFAP and an increase in vimentin immunoreactivity in brain sections. Thus, OPN may play a role in tumor progression of gliomas.

5-Aza-dC Reduces Glioma Cell Invasiveness and Growth In Vitro and In Vivo via OPN Expression

5-Aza-dC has been used to treat acute myeloid leukemia and other myelodysplastic syndromes and has also been shown to reduce human trophoblastic cell migration and

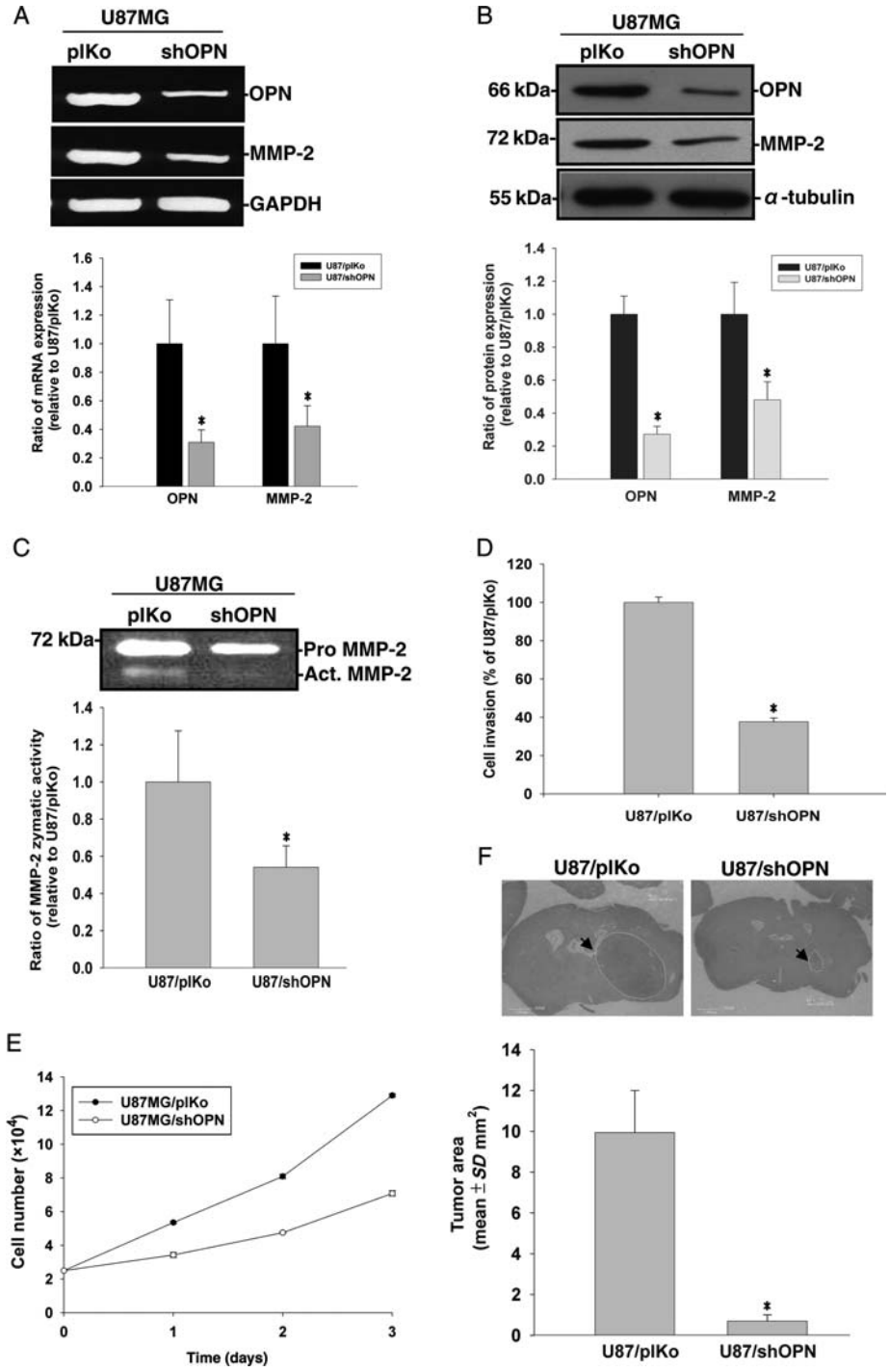

Fig. 2. U87MG cells were either stably transfected with an OPN shRNA plasmid or with a plKo shRNA vector as mock control. (A) MMP-2, OPN, and glyceraldehyde-3-phosphate dehydrogenase (GAPDH) mRNA expressions were analyzed by RT–PCR. (B) Cell lysates were harvested and immunoblotted with antibodies specific for OPN, MMP-2, and α-tubulin. These experiments were repeated, and the intensities of bands were quantitated and expressed as ratios to mock control cells. Results shown in the lower panel of (A) and (B) are the mean ± SE of three independent experiments. (C) Media were collected for the zymographic assay of MMP-2 activity. In the lower panel, MMP-2 activity was quantitated by scanning the photographic negatives on a gel analysis system. (D) For the *in vitro* invasion assay, cells were seeded in equal amounts cells in the upper part of transwell chamber separated by a Matrigel-coated membrane. Migrated cells on the bottom of the membrane were counted. Data represent the mean ± SE of three independent experiments. (E) Cells were seeded in culture plates in DMEM media supplemented with 10% heat-inactivated FCS. Viable cell numbers were counted. Data represent the mean ± SE of three independent experiments. (F) Histopathological characteristics (H&E) and tumor volumes of animals implanted with U87/plKo or U87MG/shOPN. Tumor sizes were measured through their largest diameter (upper panel), and the lower panel shows the mean ± SE of three independent experiments. $*P < .05$, compared with U87/plKo.

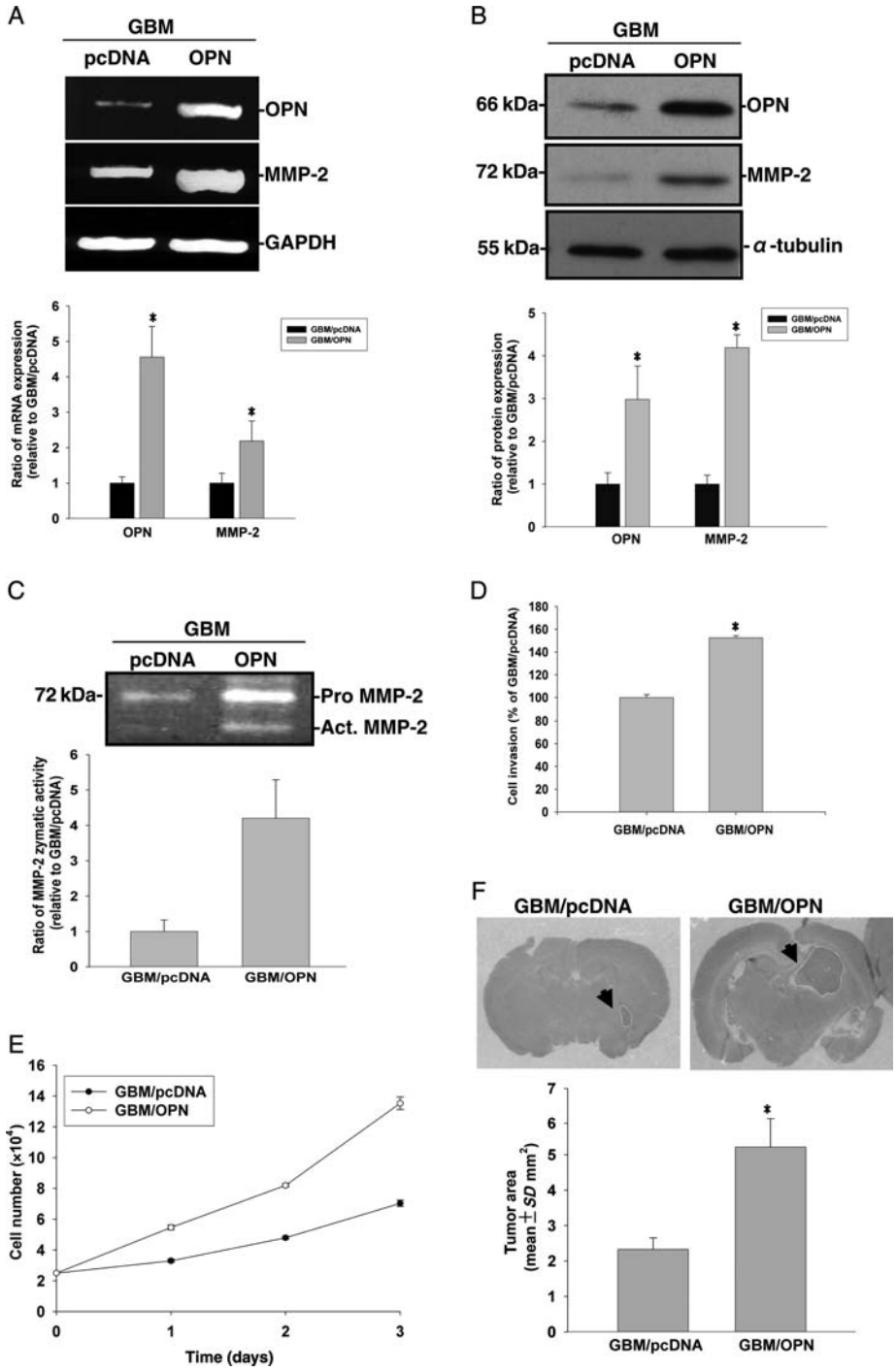

Fig. 3. GBM-SKH cells were stably expressed without or with the control vector (pcDNA3.1) or with wild-type OPN (pDNA3.1/OPN). (A) MMP-2, OPN, and glyceraldehyde-3-phosphate dehydrogenase (GAPDH) mRNA expression were analyzed by RT–PCR. (B) Cell lysates were harvested and immunoblotted with antibodies specific for OPN, MMP-2, and α-tubulin. These experiments were repeated, and the intensities of bands were quantitated and expressed as ratios to mock control cells. Results shown in the lower panel of (A) and (B) are the mean ± SE of three independent experiments. (C) Media were then collected for the zymographic assay of MMP-2 activity. In the lower panel, MMP-2 activity was quantitated by scanning the photographic negatives on a gel analysis system. (D) For the *in vitro* invasion assay, cells were seeded in equal amounts of experimental cells in the upper part of a transwell chamber separated by a Matrigel-coated membrane. Data represent the mean ± SE of three independent experiments. (E) Cells were seeded in culture plates in DMEM media supplemented with 10% heat-inactivated FCS. Viable cell numbers were counted at 24, 48, and 72 hours. Data represent the mean ± SE of three independent experiments. (F) Histopathological characteristics (H&E) and tumor volumes of animals implanted with GBM/pcDNA or GBM/OPN were evaluated. Tumor sizes were measured through their largest diameter (upper panel), and the lower panel shows the mean ± SE of three independent experiments. $*P < .05$, compared with pDNA3.1/OPN.

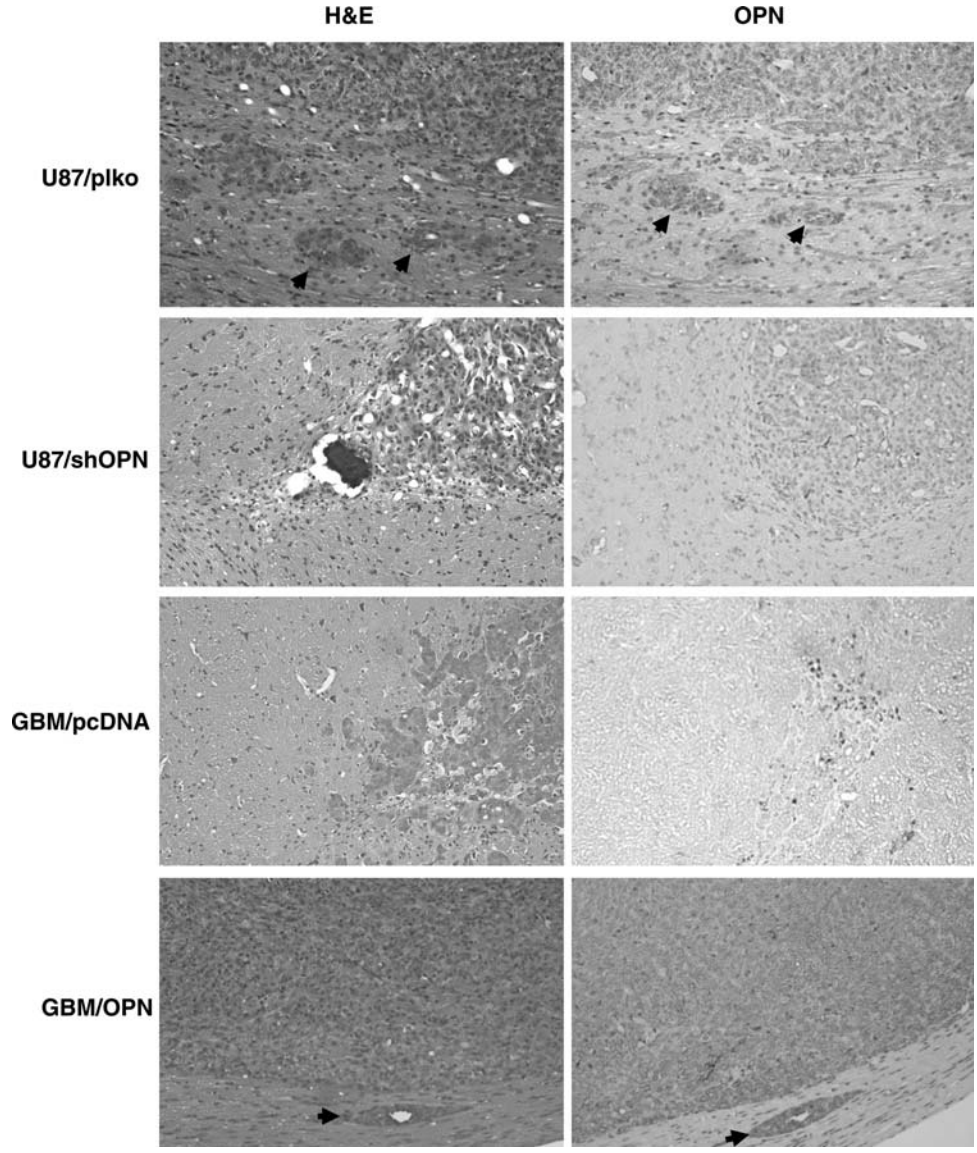

Fig. 4. U87MG cells were either stably transfected with OPN shRNA or with control shRNA; GBM-SKH cells were stably expressed with a control vector (pcDNA3.1) or with wild-type OPN (pDNA3.1/OPN). These cells were implanted into nude mice intracranially. Twenty-one days after implantation, mice were sacrificed and H&E staining and immunohistochemical analyses of OPN were performed. The arrows show the invasion of glioblastoma cells into surrounding brain tissue (left panels) and cytoplasmic OPN expression in invasive cells (right panels).

invasion.[34] Because 5-aza-dC can cross the blood-brain barrier effectively,[35] we examined whether 5-aza-dC could be used in glioma therapy. We first tested whether 5-aza-dC suppressed MMP-2 secretion in human glioma cells. Treatment of U87MG cells with 5-aza-dC for 24 hours did not alter the viability of U87MG cells as demonstrated by the MTT assay (Fig. 6B). However, incubation of glioma cells with 5-aza-dC (0–10 μM) reduced the MMP-2 gelatinolytic activity in the culture media of human glioma cells (Fig. 6A). Western blot analysis revealed that treatment with 5-aza-dC decreased OPN protein expression, which paralleled the decreased MMP-2 protein levels in U87MG cells. 5-Aza-dC has been demonstrated to induce differentiation in human hematopoietic progenitor cells.[4] We demonstrated that 5-aza-dC induced GFAP expression and decreased vimentin expression in U87MG cells (Fig. 6C). We next examined the effects of 5-aza-dC on cell invasiveness and intravasation by a Matrigel invasion assay and the chicken CAM model. The *in vitro* invasiveness through Matrigel in U87MG cells was reduced in cells treated with 5-aza-dC (Fig. 6D). Furthermore, although control U87MG cells intravasated well into the vasculature of CAM, 5-aza-dC-treated cells failed to intravasate after 4 days of incubation (Fig. 6E). Treatment with 5-aza-dC also reduced the cell proliferation rate in human glioma cells (Fig. 6F). To evaluate whether 5-aza-dC can be

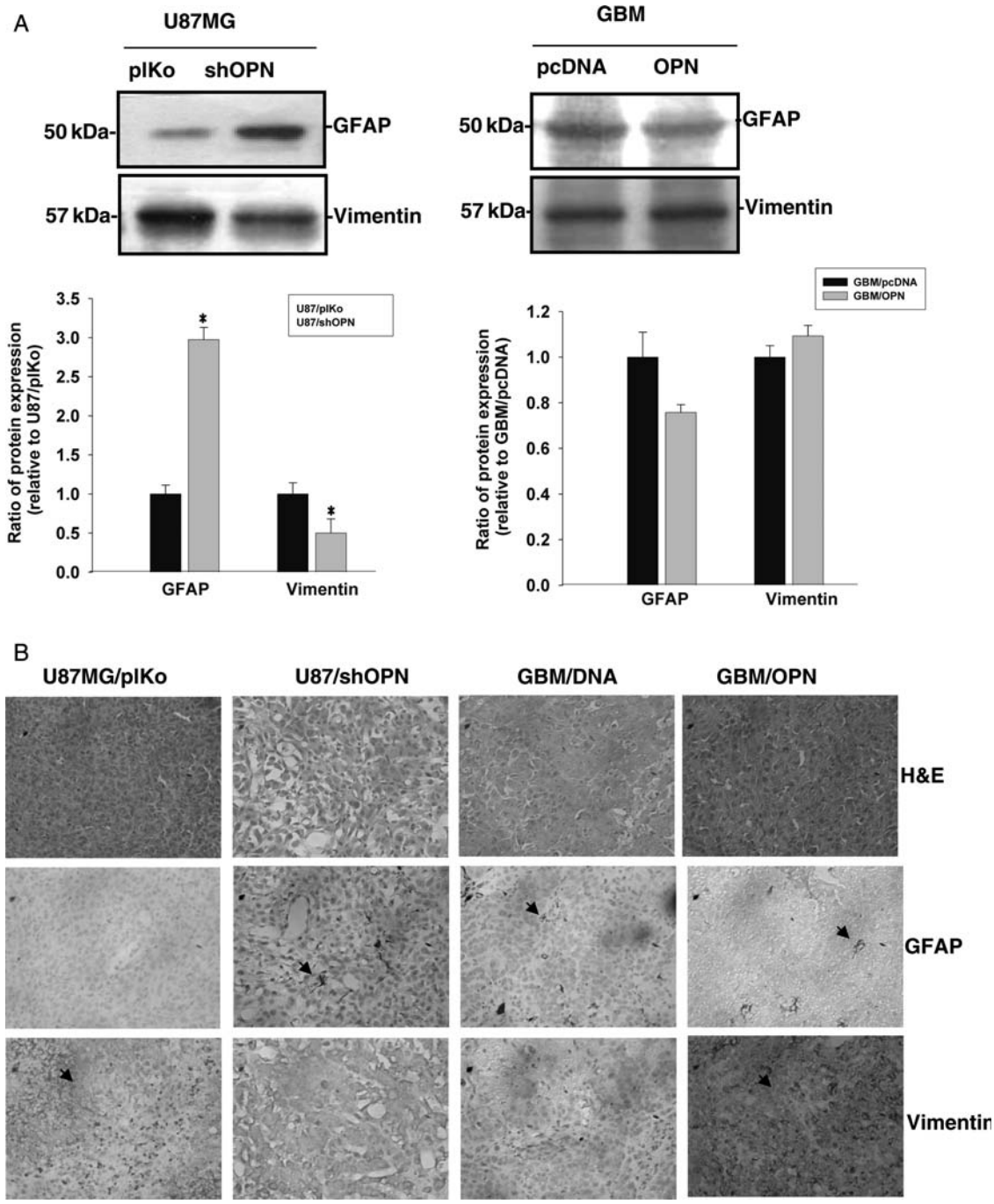

Fig. 5. OPN regulates vimentin and GFAP protein levels in glioma cells. (A) U87MG cells were stably transfected either with OPN shRNA or with control shRNA (left panel); GBM-SKH cells were stably expressed with a control vector (pcDNA3.1) or with wild-type OPN (pDNA3.1/OPN) (right panel); Cell lysates were harvested and immunoblotted with antibodies specific for GFAP and vimentin. These experiments were repeated, and the intensities of bands were quantitated and expressed as ratios to mock control cells. Results in the lower panel of (A) are the mean $\pm$ SE of three independent experiments. $^*P < .05$, compared with U87/plKo. (B) H&E staining, immunohistochemical analyses of GFAP, and vimentin in U87/plKo, U87/shOPN, GBM/pcDNA, and GBM/OPN. Mice were sacrificed and brain tissue extracted 21 days after implantation. Positive staining is indicated by arrows.

used as a therapeutic agent *in vivo*, we next examined whether an intraperitoneal injection of 5-aza-dC affected tumor growth in an intracranial xenograft model. U87MG cells (1×10^6) were transplanted into mouse brains. After implantation, mice were administered 5-aza-dC (3.75 mg/kg) or PBS at 48-hour intervals by an intraperitoneal injection. Mice were sacrificed by cardiac puncture at 21 days, and tumor volumes were evaluated microscopically in these animals. As shown in Fig. 6G, tumor size was significantly reduced in animals administered 5-aza-dC. These data suggest that 5-aza-dC can be used for glioma therapy.

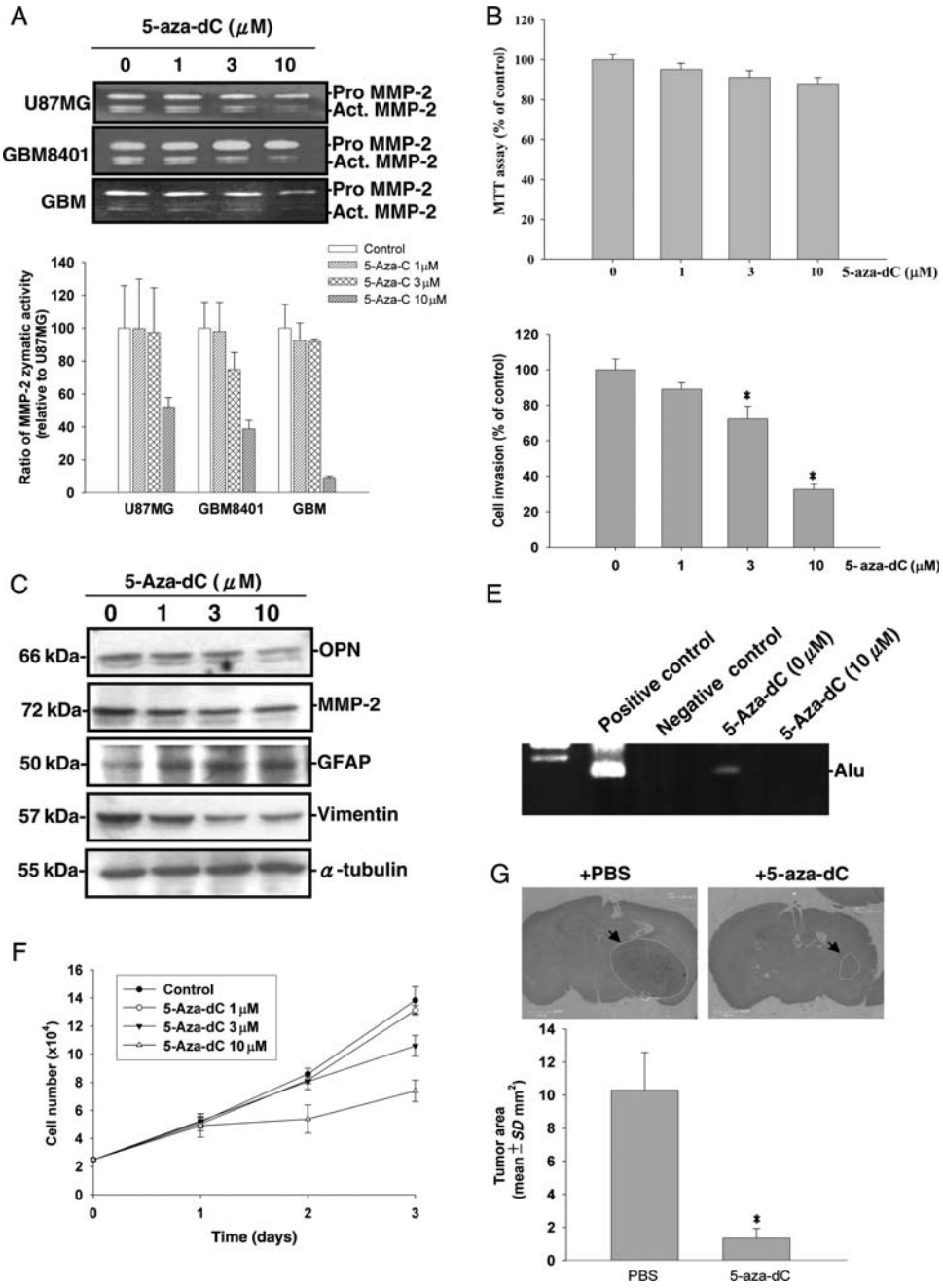

Fig. 6. Human glioma cell lines were treated with different concentrations of 5-aza-dC. (A) Media were then collected for a zymographic assay for MMP-2 activity. In the lower panel, effects of 5-aza-dC on MMP-2 secretion in various cells were quantitated by scanning the photographic negatives on a gel analysis system and are expressed as a percent of basal level for each cell line. (B) Cell viability was analyzed by the MTT assay after incubation of U87MG cells with 5-aza-dC for 24 hours. (C) Cell lysates were harvested and immunoblotted with antibodies specific for OPN, MMP-2, GFAP, vimentin, and α-tubulin. (D) For the *in vitro* invasion assay, equal numbers of glioma cells were seeded in the upper part of a transwell coated with Matrigel in the presence of different concentrations of 5-aza-dC. After 24 hours, cells on the bottom side of the filter were fixed, stained, and counted. Data represent the mean ± SE of three independent experiments. (E) An intravasation assay was carried out. PCR amplification for *Alu* sequence is shown. P, positive control; N, negative control. (F) A trypan blue exclusion assay was carried out after treating cells with different concentrations of 5-aza-dC in 5% FBS medium for different time periods. Data represent the mean ± SE of three independent experiments. (G) Measurement of implanted tumor sizes in mice without or with 5-aza-dC administration. Tumor sizes were measured through their largest diameter (upper panel), and the lower panel shows the mean ± SE of three independent experiments. $*P < .05$, compared with basal level.

Discussion

The prognosis for patients with a glioma remains dismal because current therapies fail to control gliomas from invading normal contiguous brain tissues. In the present study, we examined the capabilities of invasion and intravasation in cells isolated from two WHO grade IV glioblastoma multiforme samples and in U87MG cells. We found that cell invasiveness significantly differed among these human glioma cells. We further demonstrated that these differences may be attributed to their expression levels of OPN. This premise is supported by data where the knockdown of OPN in glioma cells decreased cell invasiveness and proliferation *in vitro* and *in vivo*, and the overexpression of OPN increased cell invasiveness and tumor growth. Additionally, we demonstrated that treatment with 5-aza-dC reduced OPN expression in U87MG cells, which resulted in a reduction in tumor size in intracranially implanted nude mice. Our results support the notion that OPN may serve as a therapeutic target and that 5-aza-dC can be used in the treatment of human malignant gliomas.

The expression of OPN has been correlated with increased tumor grade and migratory capacity of tumor cells.[13,36] We demonstrated that glioma cell lines isolated from grade IV gliomas exhibited different capabilities of tumor invasion and expressed different levels of OPN and MMP-2. We presented evidence that alteration of OPN expression levels resulted in changes in cell invasiveness and MMP-2 release. We showed that knockdown of OPN expression in highly invasive U87MG cells results in a reduction of MMP-2 expression, a decrease in cell invasion, and delayed tumor growth in mice. Consistently, overexpression of OPN in low-invasive GBM glioma cells leads to increases in MMP-2 secretion, cell invasiveness through Matrigel *in vitro*, and tumor growth *in vivo*. These results are consistent with a previous report that showed that suppression of MMP-2 gene expression may result in decreased invasiveness in malignant gliomas.[37] We extended those findings by showing that OPN is intimately linked to MMP-2 secretion, cell invasiveness, and *in vivo* tumor growth in malignant gliomas.

The expression level of GFAP is associated with glial cell differentiation and can be considered as a diagnostic marker for the differentiation of gliomas.[26] Vimentin is an intermediate filament abundantly produced in the developing central nervous system. Expression of vimentin enhances motility and the invasive potential of astrocytoma cell lines and is a marker for poorly differentiated astroglial cells.[24] In the present study, we showed that highly invasive U87MG cells express more vimentin and less GFAP. Knockdown of OPN resulted in a reduction in cell invasiveness, a decrease in vimentin expression, and an increase in the GFAP protein level. These data support the notion that OPN may regulate cell invasiveness through the expressions of vimentin and GFAP. Consistently, 5-aza-dC-reduced OPN expression, which was associated with increased GFAP and decreased vimentin expression in U87MG cells. Given that OPN may regulate MMP-2 expression and vimentin expressions, OPN can be considered a candidate target for human glioma therapy.

5-Aza-dC (Decitabine) has now been successfully advanced to clinical trials for the treatment of hematopoietic malignancies.[38] In the present study, we demonstrated that treatment of cells with 5-aza-dC suppressed MMP-2 secretion and U87MG cell invasiveness. Because 5-aza-dC is a potent inhibitor of DNA methyl transferase, DNA hypomethylation may account for the suppression of OPN expression in glioma cells. Indeed, 5-aza-dC suppresses gene expressions by unmethylating the CpGs at the upstream-activating sequences.[39,40] However, it has also been shown that 5-aza-dC may inhibit glioma invasive-growth ability through a DNA methylation-independent mechanism. The detailed mechanisms by which 5-aza-dC suppresses OPN expression are currently not clear and warrant further investigation.

In conclusion, our results suggest that OPN may play an important role in regulating MMP-2 secretion and tumor invasion. We demonstrated that an intraperitoneal injection of 5-aza-dC may suppress OPN and MMP-2 expressions and tumor growth in a rodent model. On the other hand, although temozolomide has proved to be efficacious in the treatment of human gliomas, the expression of O^6-methylguanine-DNA methyltransferase has rendered glioma cells resistant to temozolomide therapy. Given that 5-aza-dC may effectively suppress tumor growth *in vivo* and exert extra-beneficial effects in temozolomide therapy, 5-aza-dC may be considered a standard treatment regimen for glioma therapy.

Conflict of interest statement. None declared.

Funding

This work was supported by the National Science Council of Taiwan (NSC 98-3112-B038-001; NSC 97-3112-B038-002 and NSC 96-3112-B038-002), and by the Shin Kong Memorial Hospital (SKH-8302-95-DR-44).

References

1. Gunther W, Skaftnesmo KO, Arnold H, Terzis AJ. Molecular approaches to brain tumour invasion. *Acta Neurochir (Wien)*. 2003;145:1029–1036.
2. Ohgaki H. Genetic pathways to glioblastomas. *Neuropathology*. 2005;25:1–7.
3. Ohgaki H, Kleihues P. Population-based studies on incidence, survival rates, and genetic alterations in astrocytic and oligodendroglial gliomas. *J Neuropathol Exp Neurol*. 2005;64:479–489.
4. Guo Y, Engelhardt M, Wider D, Abdelkarim M, Lubbert M. Effects of 5-aza-2′-deoxycytidine on proliferation, differentiation and p15/INK4b regulation of human hematopoietic progenitor cells. *Leukemia*. 2006;20:115–121.
5. Levicar N, Nuttall RK, Lah TT. Proteases in brain tumour progression. *Acta Neurochir (Wien)*. 2003;145:825–838.

6. Rittling SR, Chambers AF. Role of osteopontin in tumour progression. *Br J Cancer*. 2004;90:1877–1881.
7. Chakraborty G, Jain S, Patil TV, Kundu GC. Down-regulation of osteopontin attenuates breast tumor progression in vivo. *J Cell Mol Med*. 2008;12(6A):2305–2318.
8. Chakraborty G, Jain S, Kundu GC. Osteopontin promotes vascular endothelial growth factor-dependent breast tumor growth and angiogenesis via autocrine and paracrine mechanisms. *Cancer Res*. 2008;68:152–161.
9. Ding Q, Stewart J, Jr, Prince CW, et al. Promotion of malignant astrocytoma cell migration by osteopontin expressed in the normal brain: differences in integrin signaling during cell adhesion to osteopontin versus vitronectin. *Cancer Res*. 2002;62:5336–5343.
10. Takano S, Tsuboi K, Tomono Y, Mitsui Y, Nose T. Tissue factor, osteopontin, alphavbeta3 integrin expression in microvasculature of gliomas associated with vascular endothelial growth factor expression. *Br J Cancer*. 2000;82:1967–1973.
11. Said HM, Hagemann C, Staab A, et al. Expression patterns of the hypoxia-related genes osteopontin, CA9, erythropoietin, VEGF and HIF-1alpha in human glioma in vitro and in vivo. *Radiother Oncol*. 2007;83:398–405.
12. Colin C, Baeza N, Bartoli C, et al. Identification of genes differentially expressed in glioblastoma versus pilocytic astrocytoma using suppression subtractive hybridization. *Oncogene*. 2006;25:2818–2826.
13. Jang T, Sathy B, Hsu YH, et al. A distinct phenotypic change in gliomas at the time of magnetic resonance imaging detection. *J Neurosurg*. 2008;108:782–790.
14. Denhardt DT, Mistretta D, Chambers AF, et al. Transcriptional regulation of osteopontin and the metastatic phenotype: evidence for a Ras-activated enhancer in the human OPN promoter. *Clin Exp Metastasis*. 2003;20:77–84.
15. Saitoh Y, Kuratsu J, Takeshima H, Yamamoto S, Ushio Y. Expression of osteopontin in human glioma. Its correlation with the malignancy. *Lab Invest*. 1995;72:55–63.
16. Urquidi V, Sloan D, Kawai K, et al. Contrasting expression of thrombospondin-1 and osteopontin correlates with absence or presence of metastatic phenotype in an isogenic model of spontaneous human breast cancer metastasis. *Clin Cancer Res*. 2002;8:61–74.
17. Philip S, Bulbule A, Kundu GC. Osteopontin stimulates tumor growth and activation of promatrix metalloproteinase-2 through nuclear factor-kappa B-mediated induction of membrane type 1 matrix metalloproteinase in murine melanoma cells. *J Biol Chem*. 2001;276:44926–44935.
18. Philip S, Kundu GC. Osteopontin induces nuclear factor kappa B-mediated promatrix metalloproteinase-2 activation through I kappa B alpha/IKK signaling pathways, and curcumin (diferulolylmethane) down-regulates these pathways. *J Biol Chem*. 2003;278:14487–14497.
19. Wai PY, Mi Z, Guo H, et al. Osteopontin silencing by small interfering RNA suppresses in vitro and in vivo CT26 murine colon adenocarcinoma metastasis. *Carcinogenesis*. 2005;26:741–751.
20. Alonso SR, Tracey L, Ortiz P, et al. A high-throughput study in melanoma identifies epithelial-mesenchymal transition as a major determinant of metastasis. *Cancer Res*. 2007;67:3450–3460.
21. Tarin D, Thompson EW, Newgreen DF. The fallacy of epithelial mesenchymal transition in neoplasia. *Cancer Res*. 2005;65:5996–6000; discussion 6000–5991.
22. Dehghani F, Schachenmayr W, Laun A, Korf HW. Prognostic implication of histopathological, immunohistochemical and clinical features of oligodendrogliomas: a study of 89 cases. *Acta Neuropathol*. 1998;95:493–504.
23. Mahesparan R, Read TA, Lund-Johansen M, Skaftnesmo KO, Bjerkvig R, Engebraaten O. Expression of extracellular matrix components in a highly infiltrative in vivo glioma model. *Acta Neuropathol*. 2003;105:49–57.
24. Rutka JT, Ivanchuk S, Mondal S, et al. Co-expression of nestin and vimentin intermediate filaments in invasive human astrocytoma cells. *Int J Dev Neurosci*. 1999;17:503–515.
25. Trog D, Fountoulakis M, Friedlein A, Golubnitschaja O. Is current therapy of malignant gliomas beneficial for patients? Proteomics evidence of shifts in glioma cells expression patterns under clinically relevant treatment conditions. *Proteomics*. 2006;6:2924–2930.
26. Jung CS, Foerch C, Schanzer A, et al. Serum GFAP is a diagnostic marker for glioblastoma multiforme. *Brain*. 2007;130:3336–3341.
27. Schmelz K, Sattler N, Wagner M, Lubbert M, Dorken B, Tamm I. Induction of gene expression by 5-Aza-2′-deoxycytidine in acute myeloid leukemia (AML) and myelodysplastic syndrome (MDS) but not epithelial cells by DNA-methylation-dependent and -independent mechanisms. *Leukemia*. 2005;19:103–111.
28. Schmelz K, Wagner M, Dorken B, Tamm I. 5-Aza-2′-deoxycytidine induces p21WAF expression by demethylation of p73 leading to p53-independent apoptosis in myeloid leukemia. *Int J Cancer*. 2005;114:683–695.
29. Waha A, Koch A, Hartmann W, et al. SGNE1/7B2 is epigenetically altered and transcriptionally downregulated in human medulloblastomas. *Oncogene*. 2007;26:5662–5668.
30. Eramo A, Pallini R, Lotti F, et al. Inhibition of DNA methylation sensitizes glioblastoma for tumor necrosis factor-related apoptosis-inducing ligand-mediated destruction. *Cancer Res*. 2005;65:11469–11477.
31. Kim J, Yu W, Kovalski K, Ossowski L. Requirement for specific proteases in cancer cell intravasation as revealed by a novel semiquantitative PCR-based assay. *Cell*. 1998;94:353–362.
32. Ma HI, Guo P, Li J, et al. Suppression of intracranial human glioma growth after intramuscular administration of an adeno-associated viral vector expressing angiostatin. *Cancer Res*. 2002;62:756–763.
33. Ma HI, Lin SZ, Chiang YH, et al. Intratumoral gene therapy of malignant brain tumor in a rat model with angiostatin delivered by adeno-associated viral (AAV) vector. *Gene Ther*. 2002;9:2–11.
34. Rahnama F, Shafiei F, Gluckman PD, Mitchell MD, Lobie PE. Epigenetic regulation of human trophoblastic cell migration and invasion. *Endocrinology*. 2006;147:5275–5283.
35. Chabot GG, Rivard GE, Momparler RL. Plasma and cerebrospinal fluid pharmacokinetics of 5-Aza-2′-deoxycytidine in rabbits and dogs. *Cancer Res*. 1983;43:592–597.
36. Jang T, Savarese T, Low HP, et al. Osteopontin expression in intratumoral astrocytes marks tumor progression in gliomas induced by prenatal exposure to N-ethyl-N-nitrosourea. *Am J Pathol*. 2006;168:1676–1685.
37. Koul D, Parthasarathy R, Shen R, et al. Suppression of matrix metalloproteinase-2 gene expression and invasion in human glioma cells by MMAC/PTEN. *Oncogene*. 2001;20:6669–6678.
38. Oki Y, Issa JP. Review: recent clinical trials in epigenetic therapy. *Rev Recent Clin Trials*. 2006;1:169–182.
39. Zhu WG, Hileman T, Ke Y, et al. 5-Aza-2′-deoxycytidine activates the p53/p21Waf1/Cip1 pathway to inhibit cell proliferation. *J Biol Chem*. 2004;279:15161–15166.
40. Fu WN, Bertoni F, Kelsey SM, et al. Role of DNA methylation in the suppression of Apaf-1 protein in human leukaemia. *Oncogene*. 2003;22:451–455.